C. R. Chimie 20 (2017) 730–737

Contents lists available at ScienceDirect

Comptes Rendus Chimie

www.sciencedirect.com

Full paper/Mémoire

Synthesis, characterization, and X-ray crystal structures of copper(I) halide and pseudohalide complexes with 2-(2-quinolyl)benzothiazole. Diverse coordination geometries and electrochemical properties

Soraia Meghdadi [a, *], Mehdi Amirnasr [a, **], Elaheh Yavari [a], Kurt Mereiter [b], Maryam Bagheri [a]

[a] Department of Chemistry, Isfahan University of Technology, Isfahan 84156-83111, Iran
[b] Faculty of Chemistry, Vienna University of Technology, Getreidemarkt 9/164SC, A-1060 Vienna, Austria

ARTICLE INFO

Article history:
Received 16 December 2016
Accepted 20 February 2017
Available online 27 March 2017

Keywords:
Benzothiazole
Copper(I) complexes
Halide and pseudohalide
X-ray structure
Cyclic voltammetry

ABSTRACT

Three new copper(I) complexes with the ligand 2-(2-quinolyl)benzothiazole (qbtz) have been synthesized and characterized by elemental analyses, infrared, and ultraviolet–visible spectroscopy, and their crystal structures have been determined by X-ray diffraction. The coordination geometry around copper in $[Cu(qbtz)(\mu\text{-}I)]_2$, complex (**1**), a centrosymmetric dimer, is a distorted CuI_2N_2 tetrahedron supplemented by a short Cu···Cu interaction of 2.5855 Å. The copper(I) cyanide–bridged complex $[Cu_3(qbtz)_2(\mu\text{-}CN)_3]$ (**2**) exhibits a one-dimensional chain structure with three crystallographically independent Cu atoms. Two of the copper atoms feature tetrahedral four coordination each by a chelating qbtz ligand and two CN groups, and the third features a quasi-linear two-coordination geometry by two CN. In [Cu(qbtz)(μ-SCN)] (**3**), copper is in a distorted tetrahedral coordination by two N atoms of a chelating qbtz ligand and by one N atom and one S atom of a bridging SCN group. The complex exhibits a one-dimensional zigzag chain structure with two crystallographically inequivalent Cu atoms in the chain. The spectroscopic and electrochemical properties of compounds **1**–**3** are in accord with the variation in copper(I) coordination environments.

1. Introduction

Copper as the third most abundant transition metal in the human body is vital for both environmental and biological systems [1,2]. Copper(I) complexes have attracted much attention because of their rich coordination chemistry and numerous catalytic and technological applications [3–9]. The copper(I) complexes of diimine ligands exhibit structural diversity and rich redox and photophysical properties [10–13] and have found important applications in bioinorganic chemistry [14,15] and for the preparation of functional materials [16–18].

Benzothiazole and its derivatives exhibit a wide range of biological activities [19] and have potential clinical applications, as antitumor [20], anticoagulant [21], antiallergic [22], anti-inflammatory [23], antimicrobial [24], and enzyme inhibitor agents [25]. The electro-optical characteristics of these materials as dopant in organic light-emitting diode devices have also been investigated [26].

In continuation of our studies on copper complexes of 2-substituted benzothiazoles [27,28], herein we report the synthesis and spectral characterization of three Cu(I) complexes of 2-(2-quinolyl)benzothiazole (qbtz) with

* Corresponding author.
** Corresponding author.
E-mail addresses: smeghdad@cc.iut.ac.ir (S. Meghdadi), amirnasr@cc.iut.ac.ir (M. Amirnasr).

http://dx.doi.org/10.1016/j.crci.2017.02.005
1631-0748/

diverse structures, namely $[Cu(qbtz)(\mu\text{-}I)]_2$ (**1**), $[Cu_3(qbtz)_2(\mu\text{-}CN)_3]$ (**2**), and $[Cu(qbtz)(\mu\text{-}SCN)]$ (**3**). The X-ray crystal structures of these complexes are reported and their cyclic voltammetric behavior is also discussed.

2. Experimental section

2.1. Materials and methods

All solvents and chemicals were of commercial reagent grade and used as received from Aldrich and Merck. Infrared (IR) spectra as KBr pellets were collected on a FT-IR JASCO 680 plus spectrometer in the range 4000–400 cm^{-1}. Ultraviolet–visible (UV–vis) absorption spectra were recorded on a JASCO V-570 spectrophotometer. Elemental analyses were performed using a Perkin Elmer 2400II CHNSO Elemental Analyzer. Electrochemical measurements were carried out at room temperature with an SAMA 500 Research Analyzer using a three-electrode system, a glassy carbon working electrode (Metrohm 6.1204.110 with 2.0 ± 0.1 mm diameter), a platinum disk auxiliary electrode, and an Ag wire as reference electrode. Cyclic voltammogram measurements were performed in DMF with tetrabutylammonium hexafluoridophosphate as the supporting electrolyte. The solutions were deoxygenated by purging with Ar for 5 min. All electrochemical potentials were calibrated versus an internal $Fc^{+/0}$ ($E^0 = 0.45$ V vs saturated calomel electrode (SCE)) couple under the same conditions [29].

2.2. Synthesis of the ligand qbtz

The ligand qbtz was prepared according to a novel procedure reported elsewhere [28] by heating a mixture of quinaldic acid and 2-aminothiophenol with triphenylphosphite in the presence of the inexpensive ionic liquid tetrabutylammonium bromide at 120 °C. The reaction was completed in 15 min. The viscous slurry obtained was treated with methanol and the resulting solid was filtered and washed with cold methanol and dried in vacuum. Yield: 87%.

2.3. Synthesis of $[Cu(qbtz)(\mu\text{-}I)]_2$(**1**)

To a solution of CuI (28.6 mg, 0.15 mmol) in acetonitrile (45 mL) was added dropwise and slowly a solution of the ligand (39.3 mg, 0.15 mmol) in acetonitrile (45 mL). The resulting yellow solution was left undisturbed at room temperature and brown crystals suitable for X-ray crystallography were obtained by slow vaporization of the solvent after 10 days. The crystals were filtered off, washed with cold acetonitrile, and dried in vacuum. Yield: 76%. Anal. Calcd for $C_{32}H_{20}I_2Cu_2N_4S_2$: C, 42.44; H, 2.23; N, 6.19; S, 7.08. Found: C, 42.52; H, 2.25; N, 6.15; S, 7.32%. FT-IR (KBr, cm^{-1}) ν_{max}: 1584 ($C{=}N_{benzothiazole}$), 1504 ($C{=}N_{quinoline}$). UV–vis: λ_{max}(nm) (ε, L mol^{-1} cm^{-1}) (DMF): 422 (380), 348 (47,180), 336 (50,300), 320 (44,440), 284 (42,840), 264 (41,380).

2.4. Synthesis of $[Cu_3(qbtz)_2(\mu\text{-}CN)_3]$ (**2**)

To a solution of $Cu(CH_3CN)_4ClO_4$ (98.2 mg, 0.30 mmol) in 90 mL of acetonitrile was added dropwise and slowly a solution of qbtz (78.6 mg, 0.30 mmol) in 90 mL of acetonitrile. To the resulting yellow solution was then added dropwise a solution of KCN (19.5 mg, 0.30 mmol) in acetonitrile (90 mL). The final solution was left undisturbed at room temperature. Orange crystals of the product suitable for X-ray crystallography were obtained after 5 days. The crystals were collected by filtration, washed with cold acetonitrile, and dried in vacuum. Yield: 72%. Anal. Calcd for $C_{35}H_{20}Cu_3N_7S_2$: C, 52.90; H, 2.54; N, 12.36; S, 8.08. Found: C, 52.82; H, 2.30; N, 12.34; S, 8.40%. FT-IR (KBr, cm^{-1}) ν_{max}: 1591 ($C{=}N_{benzothiazole}$), 1510 ($C{=}N_{quinoline}$), 2104 ($C{\equiv}N$). UV–vis: λ_{max}(nm) (ε, L mol^{-1} cm^{-1}) (DMF): 418 (358), 350 (46,100), 336 (49,750), 320 (43,420), 284 (42,020), 264 (42,950).

2.5. Synthesis of $[Cu(qbtz)(\mu\text{-}SCN)]$ (**3**)

Complex **3** was prepared by a procedure similar to that used for complex **2**, except that KSCN was used instead of KCN. Brown crystals of the product suitable for X-ray crystallography were obtained after 1 week. The crystals were collected by filtration, washed with cold acetonitrile, and dried in vacuum. Yield: 79%. Anal. Calcd for $C_{34}H_{20}Cu_2N_6S_4$: C, 53.18; H, 2.63; N, 10.94; S, 16.70. Found: C, 52.86; H, 2.58; N, 10.88; S, 16.56%. FT-IR (KBr, cm^{-1}) ν_{max}: 1588 ($C{=}N_{benzothiazole}$), 1508($C{=}N_{quinoline}$), 2094 (SCN). UV–vis: λ_{max}(nm) (ε, L mol^{-1} cm^{-1}) (DMF): 422 (376), 348 (76,300), 336 (81,260), 320 (70,980), 284 (68,260), 262 (59,530).

2.6. X-ray crystallography

X-ray data of the compounds **1**, **2**, and **3** were collected at $T = 100$ K on a Bruker Kappa APEX-II CCD diffractometer with graphite monochromated Mo Kα ($\lambda = 0.71073$ Å) radiation. Cell refinement and data reduction were performed with program SAINT [30]. Correction for absorption was carried out by the multiscan method and program SADABS [30]. The crystal structures were solved with direct methods using the program SHELXS97, and structure refinement on F^2 was carried out with the program SHELXL97 [31]. Crystal data together with other relevant information on the structure determination are summarized in Table 1. All crystal structures had in common an orientation disorder of the qbtz ligand by which the benzothiazole and the quinoline fragment switch positions so that the two sides of the *N*,*N*′-diphenylethane-1,2-diimine fragment of qbtz practically coincide and only the sulfur of the thiazole ring and a CH=CH group of the quinoline ring give separate split positions. In solid-state structures qbtz mimics thereby 2,2′-biquinoline. The proportions of major to minor qbtz orientation varied between 0.677(5) and 0.323(5) in compound **1** and 0.800(4) and 0.200(4) in compound **3**. This disorder made it necessary to apply stabilizing restraints for the most affected sites S1/S1′, C9/C9′, and C10/C10′ (unprimed/primed sites for major and minor orientation of qbtz). Further information on this aspect is provided in the deposited Crystallographic Information Files. Minor sites (S1′, C9′, C10′, and their hydrogen atoms) are not shown in the structural drawings (Figs. 1–3). The cyanide-based compound **2** showed the usual

Table 1
Crystallographic parameters, data collection, and refinement details for **1**–**3**.

Empirical formula	$C_{32}H_{20}I_2Cu_2N_4S_2$ (**1**)	$C_{35}H_{20}Cu_3N_7S_2$ (**2**)	$C_{34}H_{20}Cu_2N_6S_4$ (**3**)
Formula weight	905.52	793.32	767.88
Temperature (K)	100(2)	100(2)	100(2)
Crystal system	Triclinic	Triclinic	Monoclinic
Space group	$P\bar{1}$	$P\bar{1}$	$P2_1/n$
a (Å)	7.9721(5)	12.4075(14)	10.6396(5)
b (Å)	9.3475(5)	12.6342(14)	15.3656(8)
c (Å)	10.8772(6)	12.7497(14)	18.6910(9)
α (°)	72.934(3)	114.597(2)	90
β (°)	77.373(3)	101.217(3)	98.1187(9)
γ (°)	74.257(3)	109.392(3)	90
v (Å^3)	737.25(7)	1579.9(3)	3025.1(3)
z	1	2	4
D_{calc} (Mg/m^3)	2.040	1.668	1.686
μ (mm^{-1})	3.71	2.17	1.72
Crystal size (mm)	0.22 × 0.12 × 0.09	0.45 × 0.35 × 0.10	0.42 × 0.40 × 0.25
F(000)	436	796	1552
θ range (°)	2.3–30.0	1.9–26.4	2.4–30.0
Absorption correction	Multiscan	Multiscan	Multiscan
Reflections collected	6178	19,374	55,478
R_{int}	0.023	0.044	0.023
Data/restraints/parameters	3838/64/206	6181/153/447	8820/147/465
Goodness-of-fit on F^2	1.04	1.08	1.187
Final R indices [$I > 2\sigma(I)$][a]	$R_1 = 0.033$, $wR_2 = 0.083$	$R_1 = 0.062$, $wR_2 = 0.115$	$R_1 = 0.030$, $wR_2 = 0.0664$
Largest diff. peak and hole (e Å^{-3})	1.39 and −0.55	1.29 and −0.99	0.58 and −0.48

[a] $R_1 = \sum||F_o| - |F_c||/\sum|F_o|$, $wR_2 = \{\sum[w(F_o^2 - F_c^2)^2]/\sum[w(F_o^2)^2]\}^{1/2}$.

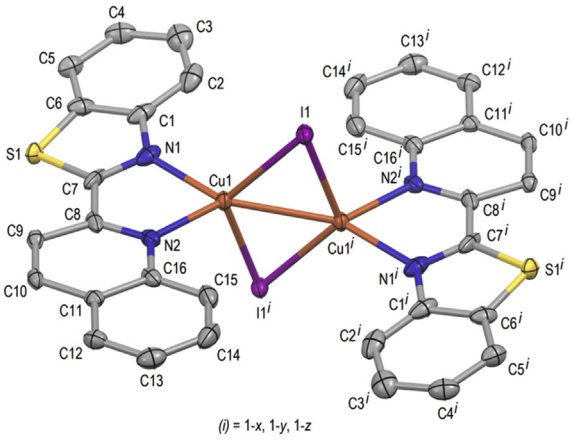

Fig. 1. View of the molecular structure of $[Cu(qbtz)(\mu\text{-}I)]_2$ (**1**) with 50% probability ellipsoids. Hydrogen atoms and additional sites for the orientation disordered qbtz ligand are omitted for clarity.

orientation ambiguity of bridging cyanides, and the cyanido groups were all treated as a superposition of pairs of CN groups with opposed orientations and occupancy factors adding up to one.

3. Results and discussion

3.1. Description of the crystal structure of $[Cu(qbtz)(\mu\text{-}I)]_2$ (*1*)

The molecular structure of complex **1** is shown in Fig. 1. The crystallographic and refinement data for **1** are summarized in Table 1, and selected bond distances and angles are listed in Table 2. Complex **1** crystallizes in the triclinic space group $P\bar{1}$ and is a neutral molecular compound consisting of centrosymmetric $Cu_2(\mu\text{-}I)_2$ units with the separation of 2.5855(8) Å between the two Cu(I) centers. This distance is close to that observed in related complexes like bis(μ-iodido)-bis(2,2′-bipyridine)-di-copper(I) (2.579 Å) [32] or bis(μ-iodido)-bis(di-2-pyridylketone)-di-copper(I) (2.547 Å) [33]. The inversion center is within the CuI_2Cu bridge. An analysis with the help of the Cambridge Structural Database [34] reveals that the Cu–Cu distances in 76 $Cu_2(\mu\text{-}I)_2$ units with N-bearing coligands vary widely between 2.51 and 3.27 Å showing a median of 2.68 Å, whereas the sum of two copper van der Waals radii is 2.80 Å (see Supplementary data for a table of the 76 structures]. Whether and to what extent a short Cu–Cu separation of 2.5855 Å within a $Cu_2(\mu\text{-}I)_2$ unit like in **1** indicates the presence of a stabilizing cuprophilic interaction remains open to question until suitable quantum-chemical calculations are available [35]. Although a tetrahedral geometry might be expected for a four-coordinated copper(I) center, the coordination sphere around the copper atom in **1** is distorted by the restricting bite angle of the chelating qbtz ligand. Disregarding the Cu…Cu interaction, the copper(I) in this complex is in a pseudotetrahedral environment with a large angular distortion, arising from the low intraligand N2–Cu1–N1 chelate angle (79.35°) that is much less than the ideal tetrahedral angle of 109.5°. On the contrary, the angles N2–Cu1–I1 (117.86°) and I1–Cu1–$I1^i$ (120.32°) are much larger than the ideal tetrahedral angle. The bond distances Cu1–N1, 2.086(3) Å, and Cu1–N2, 2.092(2) Å, are within the expected range and are comparable with those reported for related complexes (2.084(2) –2.131(3) Å for $Cu(qbtz)(PPh_3)Br/I$, [27]). The Cu–I bond distances (2.5569(4) and 2.6377(4) Å) are similar to those in related dinuclear copper (I) complexes [32–35]. The qbtz ligand is twisted by 10.6° about the bond axis C7–C8. In the crystal lattice, the dinuclear complexes are packed

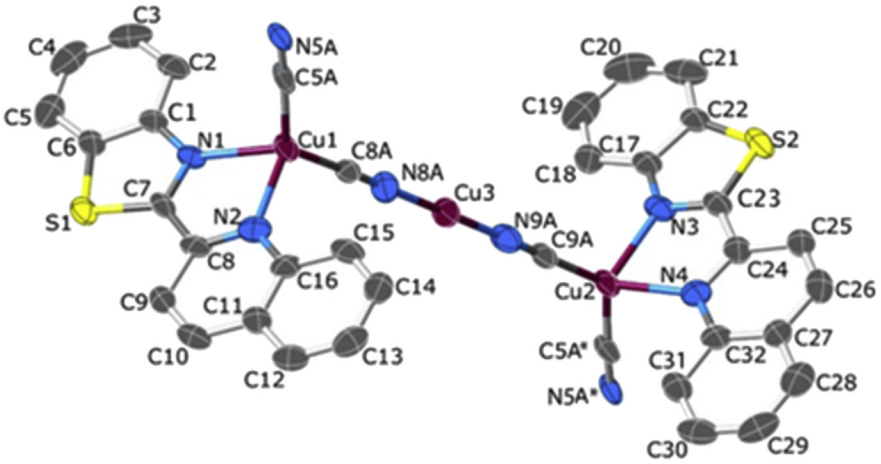

Fig. 2. The structure of $[Cu_3(qbtz)_2(\mu\text{-}CN)_3]$ with 70% probability ellipsoids. Hydrogen atoms and disordered qbtz sites are omitted for clarity. (*) Stands for the symmetry operation $(x, 1 + y, 1 + z)$.

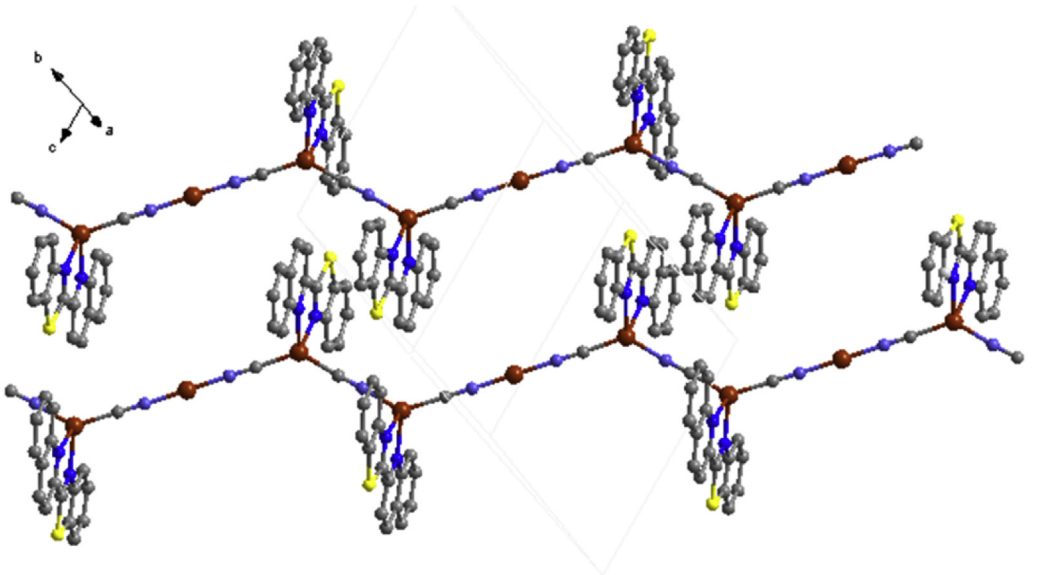

Fig. 3. Crystal packing of the $[Cu_3(qbtz)_2(\mu\text{-}CN)_3]$ complex.

Table 2
Selected bond lengths (Å) and angles (°) for **1**.

Bond lengths			
Cu1–N1	2.086(3)	Cu1–I1^{i}	2.6377(4)
Cu1–N2	2.092(2)	Cu1–Cu1^{i}	2.5855(8)
Cu1–I1	2.5569(4)	I1–I1^{i}	4.506(5)
Bond angles			
N1–Cu1–N2	79.35(12)	I1–Cu1–Cu1^{i}	61.72(2)
N1–Cu1–I1	118.12(8)	Cu1^{i}–Cu1–I1^{i}	58.61(2)
N1–Cu1–I1^{i}	106.67(7)	Cu1–I1–Cu1^{i}	59.67(2)
N2–Cu1–I1	117.83(7)	N1–Cu1–Cu1^{i}	139.35(9)
N2–Cu1–I1^{i}	107.04(7)	N2–Cu1–Cu1^{i}	139.52(9)
I1–Cu1–I1^{i}	120.32(2)		

Symmetry code: (i) $1 - x, 1 - y, 1 - z$.

approximately perpendicular to (110) by slipped π–π stacking interactions between adjacent qbtz ligands. The π–π stacking parameters are listed in Table 3.

3.2. Description of the crystal structure of $[Cu_3(qbtz)_2(\mu\text{-}CN)_3]$ (**2**)

The structure and crystal packing of complex **2** is shown in Figs. 2 and 3. Crystallographic and refinement data for **2** are summarized in Table 1, and selected bond distances and angles are listed in Table 4. Complex **2** was synthesized with the aim of obtaining Cu(CN)(qbtz) with monovalent Cu. The synthesis, however, generated $Cu_3(CN)_3(qbtz)_2$, that is, with a 3:3:2 ratio of the constituents. Of the three crystallographically independent copper atoms Cu(1) and Cu(2) feature tetrahedral four coordination by each two N atoms from the chelating qbtz ligand and two CN groups (each bridging two Cu atom). The third copper atom, Cu(3), displays a quasi-linear two coordination by two CN groups. This complex crystallizes in the space group $P\bar{1}$ and exhibits a one-dimensional chain structure with a …–Cu(qbtz)

Table 3
Aromatic interaction parameters (Å and °) for description of π–π interaction in **1**–**3**.

Cg(I)–Cg(J)	d_{Cg-Cg}[a]	$d_{plane-plane}$[b]	Slippage	Symmetry codes
Complex 1				
Cg(1)…Cg(3)	3.6514	3.4289, 3.3589		1 − *X*, −*Y*, 1 − *Z*
Cg(2)…Cg(3)	3.6622	3.3817, 3.4281		1 − *X*, −*Y*, 1 − *Z*
Cg(2)…Cg(5)	3.7511	3.3823, 3.5458		1 − *X*, −*Y*, 1 − *Z*
Cg(3)…Cg(3)	3.6816	3.3123, 3.3123	1.607	2 − *X*, −*Y*, 1 − *Z*
Cg(3)…Cg(5)	3.6675	3.3094, 3.2972		2 − *X*, −*Y*, 1 − *Z*
Cg(4)…Cg(4)	3.6856	3.5995, 3.5995	0.792	1 − *X*, −*Y*, 1 − *Z*
Complex 2				
Cg(1)…Cg(2)	3.5121	3.4595, 3.4146		1 − *X*, −*Y*, −*Z*
Cg(1)…Cg(6)	3.6147	3.2775, 3.3642		−1 + *X*, *Y*, *Z*
Cg(2)…Cg(3)	3.9532	3.4287, 3.3919		1 − *X*, −*Y*, −*Z*
Cg(2)…Cg(5)	3.5363	3.3998, 3.3651		*X*, 1 + *Y*, *Z*
Cg(3)…Cg(6)	3.6418	3.3419, 3.3527		−1 + *X*, *Y*, *Z*
Cg(4)…Cg(5)	3.6661	3.3638, 3.3543		*X*, 1 + *Y*, *Z*
Complex 3				
Cg(1)…Cg(5)	3.9935	3.6305, 3.6220		1 + *X*, *Y*, *Z*
Cg(2)…Cg(2)	3.8780	3.4318, 3.4318	1.806	1 − *X*, −*Y*, −*Z*
Cg(2)…Cg(4)	3.7353	3.4343, 3.4274		1 − *X*, −*Y*, −*Z*
Cg(3)…Cg(5)	3.8035	3.3509, 3.6356		1 + *X*, *Y*, *Z*

Complex 1: Cg(1):Cu(1)/N(1)/C(7)/C(8)/N(2); Cg(2): S(1)/C(6)/C(1)/N(1)/C(7); Cg(3): N(2)/C(8)/C(9)/C(10)/C(11)/C(16); Cg(4): C(1)/C(2)/C(3)/C(4)/C(5)/C(6); Cg(1): C(11)/C(12)/C(13)/C(14)/C(15)C(16).
Complex 2: Cg(1): S(1)/C(6)/C(1)/N(1)/C(7); Cg(2): N(2)/C(8)/C(9)/C(10)/C(11)/C(16); Cg(3): C(1)/C(2)/C(3)/C(4)/C(5)/C(6); Cg(4): C(11)/C(12)/C(13)/C(14)/C(15)/C(16); Cg(5): C(17)/C(18)/C(19)/C(20)/C(21)/C(22); Cg(6): C(27)/C(28)/C(29)/C(30)/C(31)/C(32).
Complex 3: Cg(1): S(1)/C(6)/C(1)/N(1)/C(7); Cg(2): N(2)/C(8)/C(9)/C(10)/C(11)/C(16); Cg(3): C(1)/C(2)/C(3)/C(4)/C(5)/C(6); Cg(4): C(11)/C(12)/C(13)/C(14)/C(15)/C(16); Cg(5): C(17)/C(18)/C(19)/C(20)/C(21)/C(22).
[a] Centroid–centroid distance.
[b] Perpendicular distance of Cg(I) on ring J and perpendicular distance of Cg(J) on ring I.

Table 4
Selected bond lengths (Å) and angles (°) for **2**.

Bond lengths			
Cu1–C8A	1.912(5)	Cu2–C9A	1.902(5)
Cu1–N5A	1.943(5)	Cu2–N5A	1.946(5)
Cu1–N1	2.127(5)	Cu2–N3	2.128(5)
Cu1–N2	2.160(5)	Cu2–N4	2.151(5)
Cu3–N9A	1.838(5)	Cu3–N8A	1.843(5)
Bond angles			
N1–Cu1–N2	77.28(19)	N3–Cu2–N4	77.3(2)
N1–Cu1–N5A	104.03(19)	N3–Cu2–C5A	105.8(2)
N1–Cu1–C8A	115.2(2)	N3–Cu2–C9A	113.1(2)
N2–Cu1–N5A	107.5(2)	N4–Cu2–C5A	104.27(19)
N2–Cu1–C8A	109.9(2)	N4–Cu2–C9A	111.6(2)
C5B–Cu1–C8A	130.2(2)	C5A–Cu2–C9A	131.4(2)
N8A–Cu3–N9A	179.5(3)		
Cu1–N5A–C5A$^{(i)}$	176.3(5)	Cu2–C5A–N5A$^{(i)}$	174.8(5)
Cu1–C8A–N8A	177.8(5)	Cu2–C9A–N9A	178.5(5)
Cu3–N8A–C8A	178.5(5)	Cu3–N9A–C9A	178.8(6)

Symmetry code: (i) *x*, *y* − 1, *z* − 1.

–CN–Cu(qbtz)–CN–Cu–CN–Cu(qbtz)–CN–Cu(qbtz)–… architecture practically identical with that of catena-(tris(μ_2-cyanido)-bis(2,2′-biquinoline)-tri-copper(I)) [36,37], which crystallizes in the lattice space group *C*2/*m*, however. The structure of **2** shows the usual orientational disorder (superposition of quinoline and benzothiazole) for the qbtz ligand (two independent ligands; population parameters for major/minor orientation 0.751/0.249 and 0.705/0.295). The atom coordinating a CN group to a transition metal is not invariably either C or N; moreover, we did not find any literature citation claiming that C must be bonded to the two-coordinate Cu(I) in a continuous Cu(I)–CN chain. To assess this situation in **2**, we carried out refinements including CN occupancies. These refinements yielded occupancy factors of the N-bonded (to Cu3) variety of 0.48(5), 0.88(5), and 0.85(5) for the cyanido groups N5A–C5A, N8A–C8A, and N9A–C9A, respectively. It must, however, be borne in mind that crystals of **2** were not of the splendid persuasion, and that, therefore, these occupation numbers should not be taken too literally. But in any case, there is a perceptible preference for the N bonding to Cu3, and the exclusively C-bonded CN was clearly disfavored by *R* values. A confirmation of preferred N bonding may also be found in the very similar CCDC refcode MODLOH (see the detailed discussion in the Supplementary data). The bond distances to the chelating qbtz ligand, Cu1–N1 = 2.127(5) Å, Cu1–N2 = 2.160(5) Å, Cu2–N3 = 2.128(5) Å, and Cu2–N4 = 2.151(5) Å, are within the expected range and are in agreement with those reported for related complexes (2.131(3), 2.126(3), and 2.084(2) Å) [27]. The bond angles around the tetrahedral centers Cu1 and Cu2 deviate notably from the ideal value of 109.5°, showing the smallest value of ~77° for the qbtz intraligand angle and the largest value of ~130° for the CN–Cu–CN angle, whereas the rest of the angles vary between 104 and 113° (Table 4). The atoms around the Cu3 center are defined by two cyanide ions with bond lengths of Cu3–N9A = 1.838(5) Å and Cu3–N8A = 1.843(5) Å. The bond angle around the Cu3 center is, N9A–Cu3–N8A = 179.5(3)°, close to the ideal value of 180° for a linear two coordination [36–39]. Slipped π–π stacking interactions are also observed in this complex. The π–π stacking parameters are listed in Table 3.

3.3. Description of the crystal structure of [Cu(qbtz)(μ-SCN)] (**3**)

The structure of complex **3** is shown in Fig. 4. The crystallographic and refinement data for **3** are summarized in Table 1, and selected bond distances and angles are listed in Table 5. This compound crystallizes in the monoclinic space group $P2_1/n$. The asymmetric unit of the structure contains two formula units of Cu(SCN)(qbtz). Each of the two independent copper atoms, Cu1 and Cu2, is coordinated by two N atoms of a qbtz ligand and by a N atom and a S atom of two different bridging SCN groups. Both CuN_3S coordination figures are distinctly distorted tetrahedral showing notable differences between Cu1 and Cu2 in bond lengths and bond angles as well. Main difference is that the bond angle S–Cu–N_{SCN} for Cu1 is 99.20°, whereas for Cu2 it is 121.63° (compare also N5–S4 = 3.229 Å with N6–S3^{i} = 3.676 Å, cf. Fig. 3). The Cu–N_{qbtz} mean bond length of **3** is 2.097 Å, comparable to the corresponding value of <Cu–N_{qbtz}> = 2.089 Å for **1**, but shorter than <Cu–N_{qbtz}> = 2.142 Å for **2**. The mean bond distance <Cu–N_{SCN}> = 1.924 Å is close to the <Cu–N,C> bond distance for tetrahedral Cu in **2**. Cu–S bond distances are in agreement with those reported for related complexes [27]. In the crystal lattice, complex **3** forms continuous zigzag chains along [1$\bar{0}$1] with π–π stacking interactions between the qbtz fragments of adjacent chains (Fig. 5). The π–π

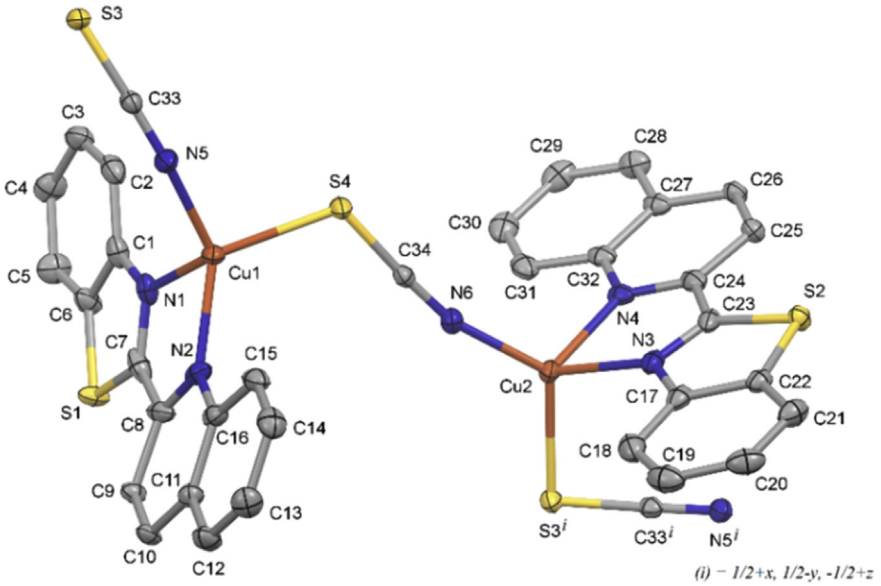

Fig. 4. View of the structure of [Cu(qbtz)(μ-SCN)] with 50% probability ellipsoids. Hydrogen atoms and disordered qbtz sites are omitted for clarity. The zigzag chain of this structure continues with Cu atoms attached to S3 and $N5^{i}$.

Table 5
Selected bond lengths (Å) and angles (°) for **3**.

Bond lengths			
Cu1–N5	1.9377(15)	Cu2–N6	1.9111(15)
Cu1–N2	2.0463(15)	Cu2–N3	2.0759(15)
Cu1–N1	2.1298(15)	Cu2–N4	2.1357(15)
Cu1–S4	2.2910(5)	$Cu2–S3^{i}$	2.2945(5)
S3–C33	1.658(2)	S4–C34	1.649(2)
C33–N5	1.160(2)	C34–N6	1.155(2)
Bond angles			
N1–Cu1–N2	79.28(7)	N3–Cu2–N4	78.62(6)
N1–Cu1–N5	110.31(7)	N3–Cu2–N6	120.67(6)
N1–Cu1–S4	115.56(4)	$N3–Cu2–S3^{i}$	103.71(4)
N2–Cu1–N5	132.78(6)	N4–Cu2–N6	111.13(6)
N2–Cu1–S4	118.58(5)	$N4–Cu2–S3^{i}$	113.32(4)
N5–Cu1–S4	99.20(5)	$N6–Cu2–S3^{i}$	121.63(5)
Cu1–N5–C33	161.76(16)	Cu2–N6–C34	164.78(15)
Cu1–S4–C34	113.81(6)	$Cu2–S3^{i}–C33^{i}$	94.17(6)

Symmetry codes: (i) $1/2 + x$, $1/2 - y$, $-1/2 + z$.

stacking parameters are listed in Table 3. Such zigzag chains are present also in the crystal structure of the 2,2′-biquinoline analogue of compound **3**, [Cu(biq)(μ-SCN)] [40], but there is only one kind of Cu that lies together with SCN on a crystallographic mirror plane bisecting the chelating biquinoline ligand (orthorhombic space group *Pnma*). The bond lengths in [Cu(biq)(μ-SCN)] [40], $Cu–N_{biq}$ = 2.107 Å, $Cu–N_{SCN}$ = 2.931 Å, and $Cu–S_{SCN}$ = 2.286 Å, are similar to **3**.

3.4. Spectral characterization

The FT-IR spectral data of the three complexes of copper are listed in Section 2. The IR spectrum of the free ligand shows two bands at 1558 and 1593 cm^{-1} characteristic of the $C{=}N_{quinoline}$ and $C{=}N_{benzothiazole}$ [27]. In the spectra of complexes the ν(C=N) is generally shifted to lower frequencies relative to the free ligand, indicating a decrease in the C=N bond order because of back bonding from the metal center to the π^* orbital of the ligand and increasing the resonance in the planar coordinated benzothiazole. The $C{=}N_{quinoline}$ and $C{=}N_{benzothiazole}$ stretching vibrations appear at 1508 and 1587 cm^{-1} for complex **1**, 1509 and 1590 cm^{-1} for complex **2**, and 1508 and 1588 cm^{-1} for complex **3**. The strong absorption band at 2104 cm^{-1} in complex **2** is assigned to the coordinated cyanido ligand [41]. The strong absorption band at 2094 cm^{-1} in complex **3** is assigned to the thiocyanato CN stretching frequencies indicating the coordination of SCN^- anion with a 1,3-μ-SCN bridging modes [41].

The UV–vis spectra of these compounds were recorded in DMF solution in the 200–800 nm region and the data are presented in Section 2. The electronic absorption spectra of complexes **1**–**3** show intense bands in the 260–441 nm region, indicating the presence of intraligand ($\pi \rightarrow \pi^*$) and charge transfer transitions. Copper(I) with d^{10} configuration is diamagnetic and no d-d electronic transition is expected for its complexes.

3.5. Electrochemical studies

The electrochemical behavior of the qtbz ligand and copper complexes has been studied by cyclic voltammetry in DMF solution at a scan rate of 100 mVs^{-1}, with 0.1 M $[N(n\text{-}Bu)_4]PF_6$ as the supporting electrolyte at a glassy carbon working electrode. The approximate concentrations of the compounds were 5×10^{-4} M. Ferrocene (Fc) was used as the internal standard, and all redox potentials are referenced to the $Fc^{+/0}$ couple [29].

The voltammogram of $[Cu(qbtz)(\mu\text{-}I)]_2$ in DMF solution is shown in Fig. 6. The anodic wave at 0.391 V and the corresponding cathodic wave observed at 0.114 V

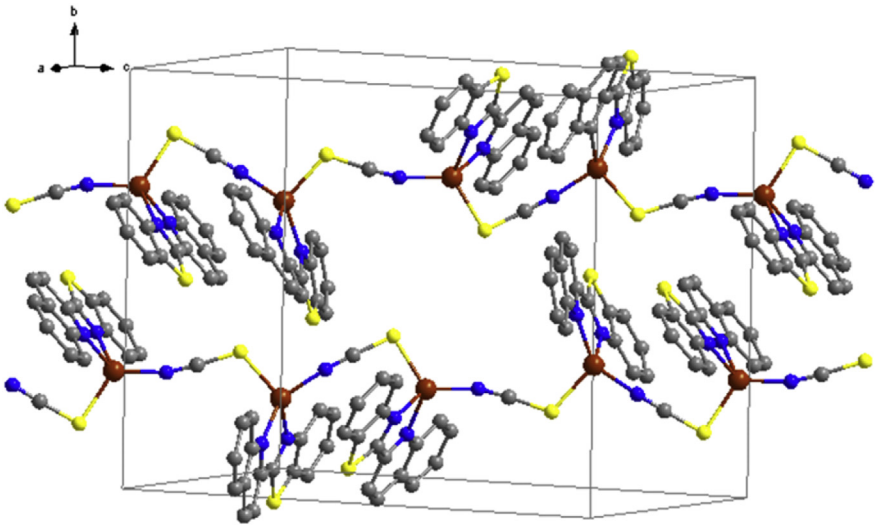

Fig. 5. Crystal packing of the [Cu(qbtz)(μ-SCN)] complex.

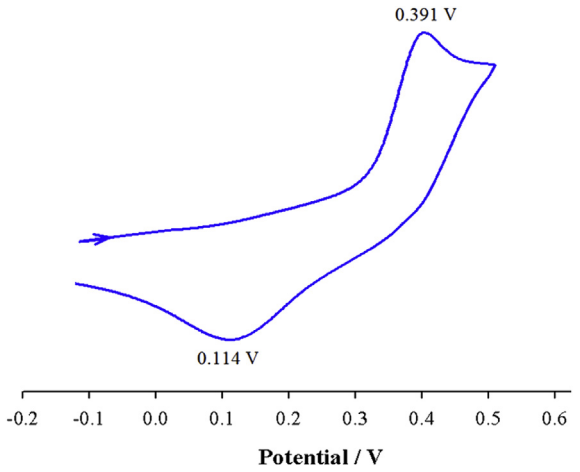

Fig. 6. Cyclic voltammogram of $[Cu(qbtz)(\mu\text{-}I)]_2$ in DMF solution at 298 K (scan rate = 100 mV s^{-1}, $c = 5 \times 10^{-4}$ M).

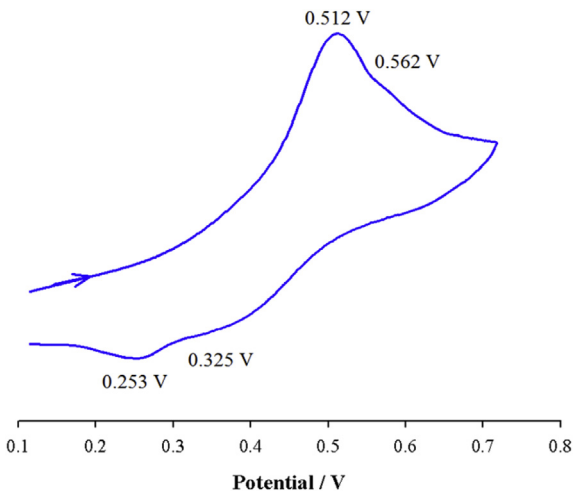

Fig. 7. Cyclic voltammogram of $[Cu_3(qbtz)_2(\mu\text{-}CN)_3]$ in DMF solution at 298 K (scan rate = 100 mV s^{-1}, $c = 5 \times 10^{-4}$ M).

(ΔE = 277 mV) are attributed to the $Cu^{I/II}$ couple undergoing an irreversible redox process and is in agreement with the values reported for related Cu(I) complexes [42].

The cyclic voltammogram of $[Cu_3(qbtz)_2(\mu\text{-}CN)_3]$ in DMF solution (Fig. 7) shows anodic waves at 0.512 and 0.562 V and the corresponding cathodic waves at 0.325 and 0.253 V and are attributed to the $Cu^{I/II}$ irreversible redox processes (ΔE = 187 and 309 mV). These observations correlate well with the existence of two types of copper centers in this complex.

The voltammogram of [Cu(qbtz)(μ-SCN)] is shown in Fig. 8. The anodic wave observed at 0.410 and the corresponding cathodic wave at 0.223 V (ΔE = 187 mV) are attributed to the irreversible redox processes of $Cu^{I/II}$ couple, which is in agreement with similar reports on Cu(I) complexes [43].

The oxidation potential of $Cu^{I/II}$, E_{pa}, in $[Cu_3(qbtz)_2(\mu\text{-}CN)_3]$ is more positive than those of **1** and **3** complexes. This

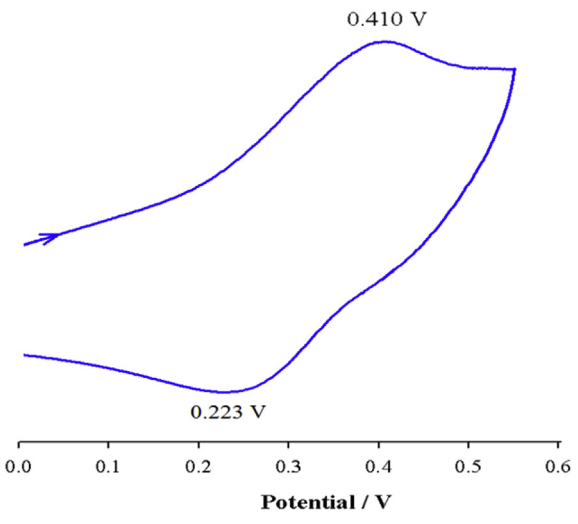

Fig. 8. Cyclic voltammogram of [Cu(qbtz)(μ-SCN)] in DMF at 298 K (scan rate = 100 mV s^{-1}, $c = 5 \times 10^{-4}$ M).

is presumably because of the stronger π-acceptor character of the CN^- relative to I^- and SCN^- ligands in the corresponding copper complexes ($I^- < SCN^- < CN^-$), which make the central metal ion harder to oxidize. The dissociation of the halide or pseudohalide ligands leading to the monomeric solvent-coordinated species may be the source of weak reduction peaks that overlap with the $Cu^{I/II}$ redox process.

4. Conclusions

This article describes the synthesis of three new multinuclear copper complexes with the bidentate ligand 2-(2-quinolyl)benzothiazole and the ancillary ligands I^-, CN^-, and SCN^-. Fully characterized, the single crystal X-ray structure analysis of these complexes shows that complex **1** is a dinuclear neutral molecular compound consisting of centrosymmetric $Cu_2(\mu\text{-}I)_2$ units. For cyanide, the synthesis generated $Cu_3(CN)_3(qbtz)_2$. Two of the three crystallographically independent Cu atoms feature tetrahedral four coordination and the third copper atom features a quasi-linear two coordination by two CN groups. This complex exhibits a one-dimensional chain structure. In complex **3** with a zigzag chain structure, the copper ion adopts a distorted tetrahedral coordination with two N atoms of the qbtz ligand and two end-on bridging thiocyanato ligands. These results indicate that the ancillary ligands contribute substantially to the structural diversity of the complexes. The Cu^I/Cu^{II} redox process is also governed by the nature of the ancillary ligands and their modes of coordination.

Acknowledgments

Partial support of this work by the Isfahan University of Technology Research Council is gratefully acknowledged. The X-ray center of the Vienna University of Technology is acknowledged for providing access to the single-crystal diffractometer.

Appendix A. Supplementary data

Supplementary data related to this article can be found at http://dx.doi.org/10.1016/j.crci.2017.02.005.

References

[1] Y. Yang, Q. Zhao, W. Feng, F. Li, Chem. Rev. 113 (2013) 192–270.
[2] S.R. Jaiser, G.P. Winston, J. Neurol. 257 (2010) 869–881.
[3] S. Rabaça, M. Almeida, Coord. Chem. Rev. 254 (2010) 1493–1508.
[4] K. Oliver, A.J.P. White, G. Hogarth, J.D.E.T. Wilton-Ely, Dalton Trans. 40 (2011) 5852–5864.
[5] K. Diwan, B. Singh, S.K. Singh, M.G.B. Drew, N. Singh, Dalton Trans. 41 (2012) 367–369.
[6] A. Kumar, R. Chauhan, K.C. Molloy, G. Kociok-Kohn, L. Bahadur, N. Singh, Chem.—Eur. J. 16 (2010) 4307–4314.
[7] S. Lal, S. Díez-González, J. Org. Chem. 76 (2011) 2367–2373.
[8] M. Liu, O. Reiser, Org. Lett. 13 (2011) 1102–1105.
[9] T. Nakamura, T. Terashima, K. Ogata, S.-i. Fukuzawa, Org. Lett. 13 (2011) 620–623.
[10] S. Singh, J. Chaturvedi, S. Bhattacharya, Dalton Trans. 41 (2012) 424–431.
[11] Z. Mao, H.-Y. Chao, Z. Hui, C.-M. Che, W.-F. Fu, K.-K. Cheung, N. Zhu, Chem.—Eur. J. 9 (2003) 2885–2894.
[12] X. Wang, C. Lv, M. Koyama, M. Kubo, A. Miyamoto, J. Organomet. Chem. 691 (2006) 551–556.
[13] T. Kern, U. Monkowius, M. Zabel, G. Knör, Eur. J. Inorg. Chem. (2010) 4148–4156.
[14] O. Lukin, F. Vögtle, Angew. Chem., Int. Ed. 44 (2005) 1456–1477.
[15] P. Mobian, J.-P. Collin, J.-P. Sauvage, Tetrahedron Lett. 47 (2006) 4907–4909.
[16] J.C. Deaton, S.C. Switalski, D.Y. Kondakov, R.H. Young, T.D. Pawlik, D.J. Giesen, S.B. Harkins, A.J.M. Miller, S.F. Mickenberg, J.C. Peters, J. Am. Chem. Soc. 132 (2010) 9499–9508.
[17] Y. Chen, J.-L. Li, G.S.M. Tong, W. Lu, W.-F. Fu, S.-W. Lai, C.-M. Che, Chem. Sci. 2 (2011) 1509–1514.
[18] M. Hashimoto, S. Igawa, M. Yashima, I. Kawata, M. Hoshino, M. Osawa, J. Am. Chem. Soc. 132 (2011) 10348–10351.
[19] J. Joseph, G. Boomadevi Janaki, J. Mol. Struct. 1063 (2014) 160–169.
[20] V. Facchinetti, R. da R. Reis, C.R.B. Gomes, T.R.A. Vasconcelos, Mini-Rev. Org. Chem. 9 (2012) 44–53.
[21] W.W. Mederski, D. Dorsch, S. Anzali, J. Gleitz, B. Cezanne, C. Tsaklakidis, Bioorg. Med. Chem. Lett. 14 (2004) 3763–3769.
[22] M.L. Richards, S.C. Lio, A. Sinha, K.K. Tieu, J.C. Sircar, J. Med. Chem. 47 (2004) 6451–6454.
[23] A.K. Verma, A. Martin, A.K. Singh Sr., Indian J. Pharm. Biol. Res. 2 (2014) 84–89.
[24] M. Singh, S.K. Singh, M. Gangwar, G. Nath, S.K. Singh, RSC Adv. 4 (2014) 19013–19023.
[25] S.T. Huang, I.J. Hsei, C. Chen, Bioorg. Med. Chem. 14 (2006) 6106–6119.
[26] M. Santra, H. Moon, M.-H. Park, T.-W. Lee, Y.K. Kim, K.H. Ahn, Chem.—Eur. J. 18 (2012) 9886–9893.
[27] S. Meghdadi, M. Amirnasr, A. Mirhashemi, A. Amiri, Polyhedron 97 (2015) 234–239.
[28] S. Meghdadi, M. Amirnasr, P.C. Ford, Tetrahedron Lett. 53 (2012) 6950–6953.
[29] N.G. Connelly, W.E. Geiger, Chem. Rev. 96 (1996) 877–910.
[30] Bruker Programs APEX2, SAINT, and SADABS, Bruker AXS Inc, Madison, Wisconsin, USA, 2008.
[31] G.M. Sheldrick, Acta Crystallogr. C71 (2015) 3–8.
[32] P.-C. Huang, K. Parthasarathy, C.-H. Cheng, Chem.—Eur. J. 19 (2013) 460–464.
[33] K.B. Szpakolski, K. Latham, C.J. Rix, J.M. White, Eur. J. Inorg. Chem. (2010) 5660–5667.
[34] For a description of CSD, see: C.R. Groom, F.H. Allen Angew. Chem., Int. Ed. 53 (2014) 662–671.
[35] X.-Y. Zhao, C.-B. Zhu, H.-P. Li, Y. Yang, H.W. Roesky, Z. Anorg. Allg. Chem. 640 (2014) 1614–1621.
[36] G. Dessy, V. Fares, P. Imperatori, G.O. Morpurgo, J. Chem. Soc., Dalton Trans. (1985) 1285–1288.
[37] D.J. Chesnut, A. Kusnetzow, R. Birge, J. Zubieta, J. Chem. Soc., Dalton Trans. (2001) 2581–2586.
[38] D.J. Chesnut, A. Kusnetzow, J. Zubieta, J. Chem. Soc., Dalton Trans. 2 (1998) 4081–4084.
[39] R.D. Pike, Organometallics 31 (2012) 7647–7660.
[40] R. Zhou, S.W. Ng, Acta Crystallogr. E62 (2006) m1691–m1692.
[41] K. Nakamoto, Infrafed and Raman Spectra of Inorganic and Coordination Compounds Part B, 6th ed., John Wiley & Sons, Inc., New York, 2009.
[42] M. Rasouli, M. Morshedi, M. Amirnasr, A.M.Z. Slawin, R. Randall, J. Coord. Chem. 66 (2013) 1974–1984.
[43] P. Kulkarni, S. Padhye, E. Sinn, C.E. Anson, A.K. Powell, Inorg. Chim. Acta 332 (2002) 167–175.